

Capacitive Response of Wigner Crystals at the Quantum Hall Plateau

Lili Zhao, Wenlu Lin, and Yang Liu*

International Center for Quantum Materials, Peking University, Haidian, Beijing, China, 100871

Y.J. Chung, K.W. Baldwin, and L.N. Pfeiffer

Department of Electrical Engineering, Princeton University, Princeton, New Jersey 08544

In this report, we study ultra-high-mobility two-dimensional (2D) electron/hole systems with high precision capacitance measurement. We find that the capacitance charge appears only at the fringe of the gate at high magnetic field when the 2D conductivity decreases significantly. At integer quantum Hall effects, the capacitance vanishes and forms a plateau at high temperatures $T \gtrsim 300$ mK, which surprisingly, disappears at $T \lesssim 100$ mK. This anomalous behavior is likely a manifestation that the dilute particles/vacancies in the top-most Landau level form Wigner crystal, which has finite compressibility and can host polarization current.

A strong perpendicular magnetic field B quantizes the kinetic energy of electrons/holes into a set of discrete Landau levels. The discrete level structure gives rise to the formation of incompressible quantum Hall liquids, an insulating phase with vanishing longitudinal conductance and quantized Hall conductance [1–3]. Another insulating phase appears when the Landau level filling factor $\nu = nh/eB$ is small [4, 5], which is generally believed to be a Wigner crystal pinned by the small but ubiquitous disorder potential [6]. In state-of-the-art high-mobility 2D systems, Wigner crystals are also seen near integer $\nu = N$ (N is a positive integer) when the particles/vacancies in the topmost Landau level have sufficiently low effective filling factors $\nu^* = |\nu - N|$. [7–9].

The capacitance is of great interest in quantum measurements [10–24]. The chemical potential μ of a Fermion system depends on its particle density, leading to the quantum capacitance that is proportional to the density of states at the Fermi energy. High sensitivity capacitance measurements can reveal fine structures of the systems' energy levels, such as the formation of delicate quantum phases [13–18], the non-parabolic dispersion [19], the interaction induced negative compressibility [20, 21], the minibands and Fermi contour transitions in multi-band 2D materials [22–24], etc. Unfortunately, quantitative studies using high precision capacitive measurement at mK-temperature are limited.

Here we report our high-precision capacitance studies on ultra-high-mobility 2D electron/hole systems at mK-temperature. We find that the device capacitance C has a strong positive dependence on the 2D longitudinal sheet conductance σ . Our observation suggests that the capacitance charge appears only at the fringe of the gate. C at integer Landau level filling factor ν approaches zero, agrees with the expectation that the zero σ prohibits charge being transported. At the vicinity of integer ν , the C plateau is seen as wide as the σ plateau at $T \simeq 300$ mK. Surprisingly, it disappears at lower temperatures while the σ plateau becomes even wider. This anomalous behavior is likely induced by the

Wigner crystal formed by the dilute particles/vacancies in the topmost Landau level.

The samples used in this study are made from GaAs wafers grown by molecular beam epitaxy along the (001) direction. These wafers consist of GaAs quantum well bounded on either side symmetrically by undoped Al-GaAs spacer layers and δ -doping layers. Samples A and B are Si-doped electron systems with 30-nm-wide quantum well and as-grown density $n \simeq 2.0 \times 10^{11} \text{ cm}^{-2}$. Sample C is C-doped hole system with 17.5-nm-wide quantum well and as-grown density $p \simeq 1.6 \times 10^{11} \text{ cm}^{-2}$. Each sample has alloyed InSn or InZn contacts at the four corners of a $2 \times 2 \text{ mm}^2$ piece cleaved from the wafer. For each sample, we evaporate several separate Au/Ti front gates

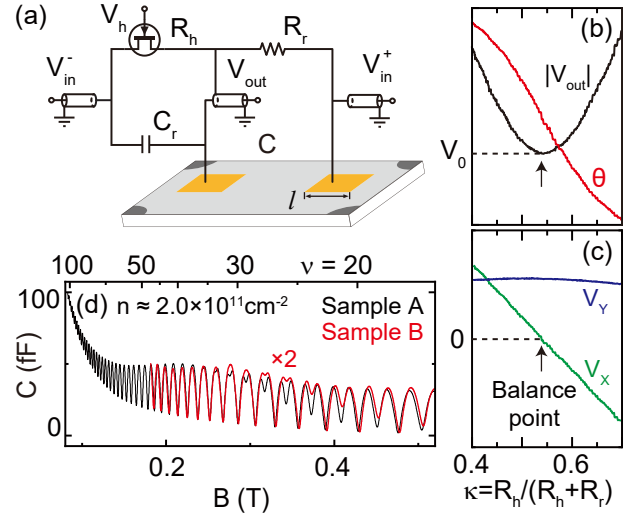


FIG. 1. (a) Circuit diagram of our capacitive measurement setup. (b) The measured amplitude and phase of output signal. $|V_{\text{out}}|$ reaches its minimum V_0 and $\theta = -\pi/2$ when the bridge is at balance point, indicated by the black arrows. (c) V_{out} can be separated into the in-phase and out-of-phase components, $V_X = |V_{\text{out}}| \cdot \cos\theta$ and $V_Y = |V_{\text{out}}| \cdot \sin\theta$. (d) The C vs. B taken from samples A (black) and B (red). The red trace is amplified by a factor of 2.

with different geometries, and measure the gate-to-gate capacitance. Samples A & B consist 500 μm -separated square gates with $l = 200$ and $100 \mu\text{m}$, respectively (Fig. 1(b)). Sample C consists concentric gates (Fig. 3(b) inset). The inner gate radius is $60 \mu\text{m}$, and the gap between the two gates is $20 \mu\text{m}$. We have compared samples with different gate geometries, and find that the observed features have no substantial dependence on the gate geometry (data not shown). The measurements are carried out in a dilution refrigerator with base temperature $T \simeq 30 \text{ mK}$.

Figure 1 depicts the principle of our measurement [25]. The passive bridge installed at the sample stage consists one resistance arm and one capacitance arm. The resistance arm includes a reference resistance R_r and one voltage-controlled-variable-resistance R_h , implemented by the source-to-drain resistance of a high-electron-mobility-transistor. We tune R_h via the transistor's gate voltage V_h , and measure R_h and R_r in-situ with low-frequency lock-in technique. We excite the bridge with a radio-frequency voltage (typically $\simeq 130 \text{ MHz}$, $\simeq 0.5 \text{ mV}_{\text{PP}}$). We amplify the bridge output V_{out} and measure its amplitude and phase with a custom-built radio-frequency lock-in amplifier. The measured $|V_{\text{out}}|$ reaches minimum value V_0 when the bridge is balanced, e.g. $R_h/R_r = C/C_r$, see Fig. 1(b). By properly choosing the reference phase, we can separate V_{out} into the in-phase and out-of-phase components V_X and V_Y . $V_X = 0$ when the bridge is balanced and has a linear dependence on $\kappa = R_h/(R_h + R_r)$ with slope $S = \partial V_X/\partial \kappa$, see Fig. 1(c). $V_Y \simeq V_0$ is nearly independent on κ . At the vicinity of the balance point, we can also deduce the C from the approximation $V_X = -S \cdot (\frac{C}{C+ C_r} - \kappa)$, which agrees with the value measured by balancing the bridge, see Fig 2(b).

The C data in Fig. 1(d) appreciates the merit of our high precision measurement. As B increases, C decreases dramatically from its $B = 0$ value (which is close to the estimated geometric capacitance of a few pF) by orders of magnitude [26]. Similar phenomenon has been reported in previous experiments where the screening capability of high quality 2D reduces significantly at high field [21]. The shrinking of C is less violent in samples which has shorter scattering time or smaller size, or when we use lower measurement frequencies, also consistent with other studies [12, 13, 15]. In Fig. 1(d), we compare data taken from samples A & B, whose gate dimensions differ by a factor of 2 and center-to-center distances are kept the same. In both samples, the capacitance oscillation starts at $B \lesssim 0.01 \text{ T}$ when $\nu \gtrsim 150$, evidencing that our measurement is as gentle as DC transport. Interestingly, the traces taken from two samples are nearly a replica of each other but scales by a factor of 2.

We can understand these features with the model shown in Fig. 2(a). The 2D system is grounded through contacts remote from the gates. A time-varying voltage $V_0 \cdot e^{i\omega t}$ applied on the gate induces an oscillating

capacitance charge density $Q(\mathbf{r}) \cdot e^{i\omega t}$ in the 2D system satisfying $Q(\mathbf{r}) = -\frac{\epsilon}{d}(V_0 + \mu(\mathbf{r})/q)$, where ϵ is the dielectric constant, d is the gate-to-2D distance, $q = \pm e$ is the particle's charge and $\mu(\mathbf{r})$ is the local chemical potential of the 2D system. For simplicity, we neglect the time-dependence term $e^{i\omega t}$ and replace $\partial/\partial t$ with $i\omega$ in the following text. The spatial variation of $\mu(\mathbf{r})$ generates a current distribution $\mathbf{j}(\mathbf{r}) = \frac{\sigma}{q}\nabla\mu(\mathbf{r})$ in the 2D system and by the charge conservation law, $\nabla \cdot \mathbf{j}(\mathbf{r}) = i\omega \cdot Q(\mathbf{r})$.

At high field when $\omega_C\tau \gg 1$, ω_C is the particles' cyclotron frequency and τ is their scattering time, the σ of an ultra-high mobility 2D system vanishes as $\sigma \simeq \sigma_{(B=0)}/(1 + (\omega_C\tau)^2)$. $\nabla\mu(\mathbf{r})$ is almost zero except at the proximity of the gate boundary, and $\mu(\mathbf{r}) \approx qV_0$ at the center of the gate. Near this edge, $Q(\mathbf{r}) \propto \pm \exp(-|d|/\xi)$ where d is the distance from the boundary and $\xi = \sqrt{\sigma d/(\omega\epsilon)}$. Furthermore, the current induced potential change outside the gated region as well as the parasitic capacitance C_P become non-negligible when σ is small. Combining all above effects, the $C = \int Q(\mathbf{r})d\mathbf{r}/V_0$ is proportional to the length of the gate perimeter and reduces as B^{-3} , see the numerical results in Fig. 2(c). We show C measured in 2D electron and hole samples with differ-

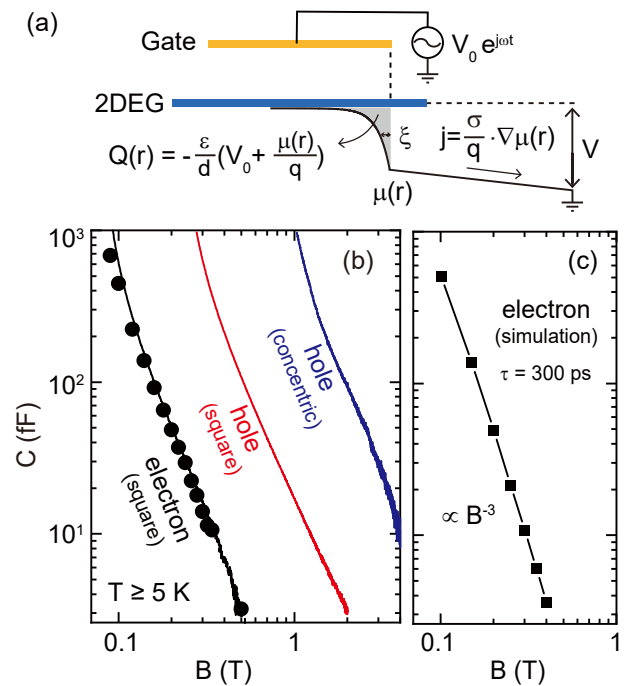


FIG. 2. (color online) (a) The model describing the capacitance response of our device. The AC voltage applied to the gate varies the chemical potential $\mu(\mathbf{r})$ of the underlying 2D system, inducing a capacitance charge density $Q(\mathbf{r})$ and corresponding current density $\mathbf{j}(\mathbf{r})$. (b) C measured from three different samples at high temperatures $T \geq 5 \text{ K}$. The symbols represent C deduced from the balance condition and the lines are results converted from V_X . (c) Numerical simulation predicts the $C \propto B^{-3}$ dependence. We use $\tau=300 \text{ ps}$ to match with the Fig. 2(b) electron data.

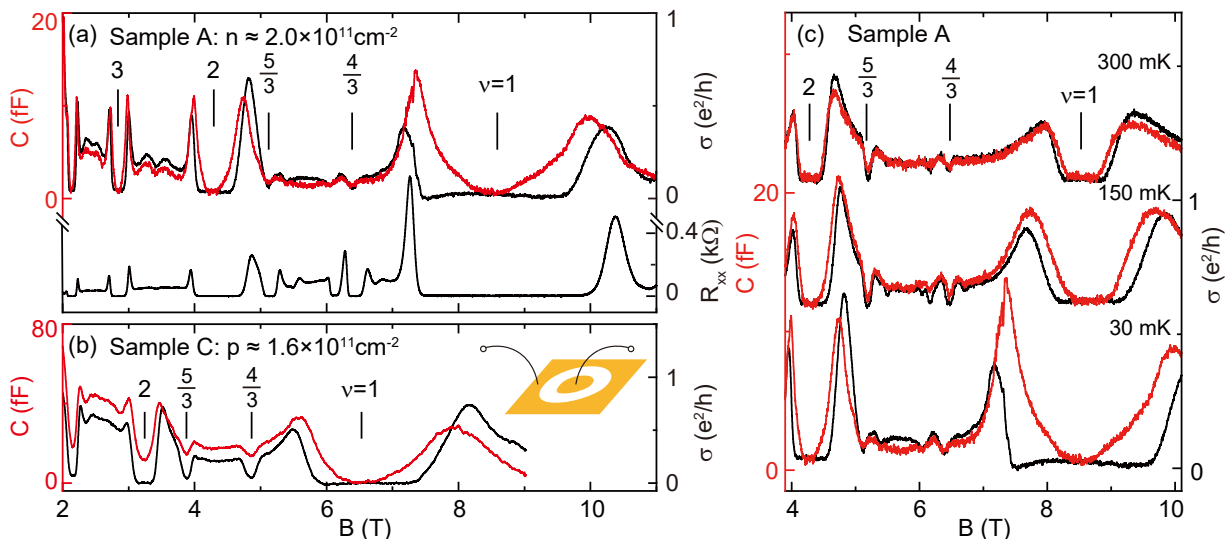


FIG. 3. (color online) (a) C , σ and the longitudinal resistance R_{xx} taken from sample A. (b) C , σ taken from sample C. (c) C and σ taken from sample A at different temperatures. Traces are offset vertically.

ent gate geometries in Fig. 2(b). The measured C is in nearly perfect agreement with the B^{-3} prediction. This model also predicts that C decreases slower if τ is smaller or the effective mass is larger, also consistent with our observation in Fig. 2(b) where C in 2D hole systems is usually higher than in 2D electron systems at high field.

Based on the Fig. 2 model, the out-of-phase signal V_Y is a good measure of σ , where $V_Y = V_0 - S \cdot (\frac{\sigma}{\sigma + \omega C_T} - \kappa)$ if $\omega C_T \tau \gg 1$. Fig. 3(a) shows the deduced σ and the R_{xx} of sample A obtained from the in-situ quasi-DC transport measurement using the four corner contacts. Both σ & R_{xx} traces have wide, flat plateaus when the 2D system form incompressible integer quantum Hall insulator at $\nu = 1, 2, 3$, etc. We also notice that C and σ are remarkably similar with each other. This may not be surprising since the Fig. 2 model predicts that C strongly entangles with σ . Mysteriously, no plateau is seen in the C trace at integer fillings while one would expect vanishing C when $\sigma = 0$. The missing plateau in C is substantiated by the Fig. 3(b) data, taken from sample C which is a 2D hole system with concentric gate geometry.

The Fig. 3(c) data taken from sample A at 30, 150 and 300 mK is even more intriguing. At the highest temperature $T \simeq 300$ mK, the C and σ traces are almost exact replica of each other. Both of them have well-developed plateau at $\nu = 1$ and 2, a manifestation that the 2D system form quantum Hall insulator and the extra particles/holes at the vicinity of $\nu = 1$ and 2 are localized and cannot response to external electric field. When the 2D system becomes colder, the C remains zero at exact integer fillings $\nu = 1$ and 2, but its plateau gradually becomes narrower and eventually disappears at $\simeq 30$ mK while the σ plateau broadens.

The fact that C becomes finite at low temperatures

while $\sigma = 0$ suggests that charge can still be effectively transported in-plane while the 2D system is not conducting. Plateaus appear near $\nu = 1$ and 2 in the high-temperature trace when the system exhibits incompressible quantum Hall insulators, because that the extra particles/vacancies are localized and cannot response to the AC voltage. Surprisingly, C becomes finite at low temperature when the localization is expected to be stronger.

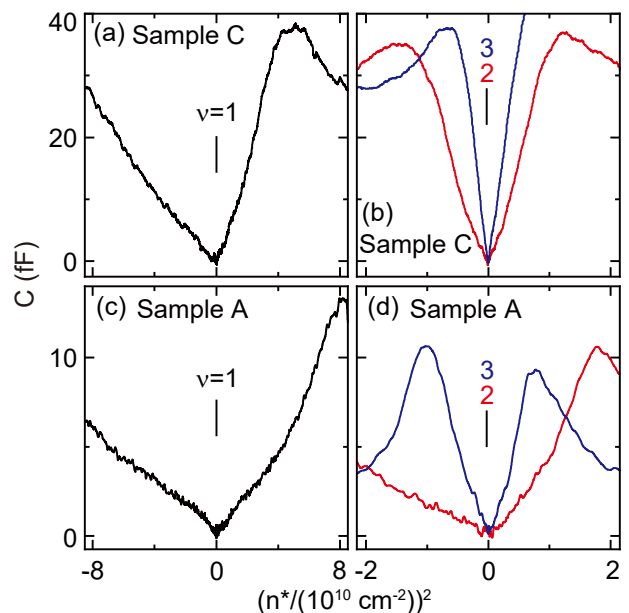


FIG. 4. (color online) (a & b) C taken from sample C near $\nu = 1, 2$ and 3 as a function of $(n^*)^2$. The negative $(n^*)^2$ represents data from $\nu^* < 1$ while the positive $(n^*)^2$ is data from $\nu^* > 1$. (c & d) C vs. $(n^*)^2$ near $\nu = 1, 2$ and 3, taken from sample A.

One plausible explanation is the existence of a long-range correlated compressible phase which is stable only at low temperatures. It has been suggested by previous studies that the dilute particles/vacancies in the topmost Landau level may form a Wigner crystal at the vicinity of integer filling factors [7]. This solid phase cannot host conducting current, but its deformation in time-varying external electric field generates polarization current. The finite C is an outcome of the finite compressibility of this Wigner crystal. In such a scenario, C approaching zero at $T \gtrsim 200$ mK signals the melting of the Wigner crystal.

We investigate the capacitive response of the Wigner crystal quantitatively in Fig. 4. Figs. 4(a) & (b) show data taken from the sample C near $\nu = 1, 2$ and 3. The capacitance C has a linear dependence on $(n^*)^2$, where $n^* = \frac{\nu^*}{\nu} n$ is the density of particles/vacancies that form the Wigner crystal. Such linear C vs. $(n^*)^2$ dependence is also seen in the electron sample near $\nu = 2$ and 3 (Fig. 4(d)). However, data taken from the electron sample near $\nu = 1$ has a skewed ' ν '-shape (Fig. 4(c)). This could be possibly related to electrons' small spin splitting. We also notice that the C vs. $(n^*)^2$ in Fig. 4(a) is quite asymmetric for positive and negative n^* , while the traces in Fig. 4(b) are more-or-less symmetric. The slope $|\partial C/\partial((n^*)^2)|$ at positive $n^* > 0$ is about 3-times larger than the negative $n^* < 0$ side. This might be because that the $n^* > 0$ ($n^* < 0$) Wigner crystals are formed by particles (vacancies) in different Landau levels, and have different compressibility. The intriguing experimental observations of Wigner crystals in Fig. 4 call for future theoretical and experimental investigations.

In conclusion, with the help of our high-precision capacitance measurement setup, we carefully study the capacitance response of ultra-high mobility 2D systems at mK temperature. Our result shows that the device capacitance strongly entangles with the 2D conductivity σ and vanishes if $\sigma = 0$. Surprisingly, at the $\sigma = 0$ plateau of integer quantum Hall effects, C is only zero at high temperatures but becomes finite at base temperature. This anomalous behavior is consistent with the formation of compressible Wigner crystal which can response to AC voltage through polarization current. Our experimental result suggests that this response depends on the Wigner crystal density n^* as $C \propto (n^*)^2$.

We acknowledge support by the NSFC (Grant No. 92065104 and 12074010) for sample fabrication and measurement, and the NSF (Grants DMR-1305691, and MRSEC DMR-1420541), the Gordon and Betty Moore Foundation (Grant GBMF4420), and Keck Foundation for the material growth. We thank M. Shayegan, Xin Wan, Bo Yang, Wei Zhu for valuable discussion.

- [1] R. E. Prange and S. M. Girvin, eds., *The Quantum Hall Effect* (Springer, New York, 1987).
- [2] S. D. Sarma and A. Pinczuk, eds., *Perspectives in Quantum Hall Effects* (Wiley, New York, 1997).
- [3] J. K. Jain, *Composite Fermions* (Cambridge University Press, Cambridge, UK, 2007).
- [4] H. W. Jiang, R. L. Willett, H. L. Stormer, D. C. Tsui, L. N. Pfeiffer, and K. W. West, *Phys. Rev. Lett.* **65**, 633 (1990).
- [5] V. J. Goldman, M. Santos, M. Shayegan, and J. E. Cunningham, *Phys. Rev. Lett.* **65**, 2189 (1990).
- [6] See articles by H. A. Fertig and by M. Shayegan, in *Perspectives in Quantum Hall Effects*, Edited by S. Das Sarma and A. Pinczuk (Wiley, New York, 1997).
- [7] Y. Chen, R. M. Lewis, L. W. Engel, D. C. Tsui, P. D. Ye, L. N. Pfeiffer, and K. W. West, *Phys. Rev. Lett.* **91**, 016801 (2003).
- [8] Y. Liu, C. G. Pappas, M. Shayegan, L. N. Pfeiffer, K. W. West, and K. W. Baldwin, *Phys. Rev. Lett.* **109**, 036801 (2012).
- [9] A. T. Hatke, Y. Liu, B. A. Magill, B. H. Moon, L. W. Engel, M. Shayegan, L. N. Pfeiffer, K. W. West, and K. W. Baldwin, *Nature Communications* **5**, 4154 (2014).
- [10] M. Kaplit and J. N. Zemel, *Phys. Rev. Lett.* **21**, 212 (1968).
- [11] A. M. Voshchenkov and J. N. Zemel, *Phys. Rev. B* **9**, 4410 (1974).
- [12] T. P. Smith, B. B. Goldberg, P. J. Stiles, and M. Heiblum, *Phys. Rev. B* **32**, 2696 (1985).
- [13] V. Mosser, D. Weiss, K. Klitzing, K. Ploog, and G. Weimann, *Solid State Communications* **58**, 5 (1986).
- [14] R. C. Ashoori, H. L. Stormer, J. S. Weiner, L. N. Pfeiffer, S. J. Pearton, K. W. Baldwin, and K. W. West, *Phys. Rev. Lett.* **68**, 3088 (1992).
- [15] T. P. Smith, W. I. Wang, and P. J. Stiles, *Phys. Rev. B* **34**, 2995 (1986).
- [16] M. J. Yang, C. H. Yang, B. R. Bennett, and B. V. Shanabrook, *Phys. Rev. Lett.* **78**, 4613 (1997).
- [17] J. P. Eisenstein, L. N. Pfeiffer, and K. W. West, *Phys. Rev. B* **50**, 1760 (1994).
- [18] A. A. Zibrov, C. Kometter, H. Zhou, E. M. Spanton, T. Taniguchi, K. Watanabe, M. P. Zaletel, and A. F. Young, *Nature* **549**, 360 (2017).
- [19] H. Irie, T. Akiho, and K. Muraki, **12**, 063004 (2019).
- [20] J. P. Eisenstein, L. N. Pfeiffer, and K. W. West, *Phys. Rev. Lett.* **68**, 674 (1992).
- [21] H. Deng, L. N. Pfeiffer, K. W. West, K. W. Baldwin, L. W. Engel, and M. Shayegan, *Phys. Rev. Lett.* **122**, 116601 (2019).
- [22] J. Jo, E. A. Garcia, K. M. Abkemeier, M. B. Santos, and M. Shayegan, *Phys. Rev. B* **47**, 4056 (1993).
- [23] A. A. Zibrov, P. Rao, C. Kometter, E. M. Spanton, J. I. A. Li, C. R. Dean, T. Taniguchi, K. Watanabe, M. Serbyn, and A. F. Young, *Phys. Rev. Lett.* **121**, 167601 (2018).
- [24] S. L. Tomarken, Y. Cao, A. Demir, K. Watanabe, T. Taniguchi, P. Jarillo-Herrero, and R. C. Ashoori, *Phys. Rev. Lett.* **123**, 046601 (2019).
- [25] Lili Zhao, *et al.*, to be published.
- [26] In all samples, our measured capacitance approaches a constant value $\simeq 60$ fF when the particles forms incompressible integer quantum Hall liquid. This is likely the parasitic capacitance C_P induced by the bonding wires, gates, etc. We have subtracted this value in all figures.

* liuyang02@pku.edu.cn